LANGMUIR Cite This: *Langmuir* 2018, 34, 147−153 Article pubs.acs.org/Langmuir

High-Speed but Not Magic: Microwave-Assisted Synthesis of Ultra-Small Silver Nanoparticles

Patrick E. J. Saloga,[†] Claudia Kästner,[†] and Andreas F. Thünemann*

Federal Institute for Materials Research and Testing (BAM), Unter den Eichen 87, 12205 Berlin, Germany

ABSTRACT: Reaction procedures have been improved to achieve higher yields and shorter reaction times: one possibility is the usage of microwave reactors. In the literature, this is under discussion, for example, nonthermal effects resulting from the microwave radiation are claimed. Especially for the synthesis of nanomaterials, it is of crucial importance to be aware of influences on the reaction pathway. Therefore, we compare the syntheses of ultra-small silver nanoparticles via conventional and microwave heating. We employed a versatile one-pot polyol synthesis of poly(acrylic acid)-stabilized silver nanoparticles, which display superior catalytic properties. No microwave-specific effects in terms of particle size distribution characteristics, as derived by small-angle X-ray scattering and dynamic light scattering, are revealed. Because of the characteristics of a closed system, microwave reactors give access to elevated temperatures and pressures. Therefore, the speed of particle formation can be increased by a factor of 30 when the reaction temperature is increased from 200 to 250 °C. The particle growth process follows a cluster coalescence mechanism. A postsynthetic incubation step at 250 °C induces a further growth of the particles while the size distribution broadens. Thus, utilization of microwave reactors enables an enormous decrease of the reaction time as well as the opportunity of tuning the particle size. Possibly, decomposition of the stabilizing ligand at elevated temperatures results in reduced yields. A compromise between short reaction times and high yields can be found at a temperature of 250 °C and a corresponding reaction time of 30 s.

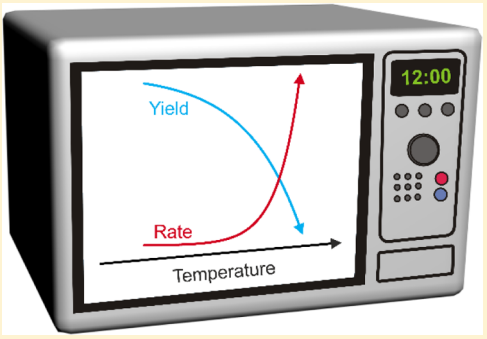

INTRODUCTION

The use of microwave irradiation has become very popular for the synthesis of nanoparticles including silver nanoparticles.[1−4] The main advantage of using a microwave for synthesis is a dramatic reduction of the overall processing time because of the available high heating rates. Within this respect, a time-saving synthesis of silver nanoparticles by using microwave irradiation is obviously of interest for scientific as well as for industrial reasons. However, in the literature, the influence of microwave radiation on the particle formation mechanism is under controversial discussion.[1] A main aspect of the ongoing dispute is related to the formation of hot spots, which could alter the reaction pathway.[5]

To clarify whether microwave radiation affects the reaction outcome with so-called "specific" or "nonthermal" microwave effects,[1] this study is aimed to provide a direct comparison of conventional and microwave heating-based syntheses of silver nanoparticles. The comparison was performed by using the same conditions for both, that is, reactants, temperature, reaction time, and vessel material. Finally, we want to provide a fast and reliable synthesis procedure for production of ultra-small silver nanoparticles with a narrow size distribution by employing a versatile polyol process.[6] The particles of interest consist of a silver core and a polymeric shell of poly(acrylic acid) (PAA) and display a superior catalytic activity in the reduction of 4-nitrophenol to 4-aminophenol.[7] We employed small-angle X-ray scattering (SAXS) to obtain the distribution of the core radii. The hydrodynamic radii including the shell and the core were determined by multiangle dynamic light scattering (DLS).

The synthesis of silver nanoparticles in the present work was performed in ethylene glycol first at its boiling point of 200 °C for direct comparison of conventional and microwave-assisted syntheses. Second, we used higher temperatures and pressures in the microwave reactor, which cannot be reached in conventional synthesis, because of the solvent's boiling point.

EXPERIMENTAL SECTION

Materials. All chemicals were used as received without further purification. Silver nitrate was purchased from AppliChem, PAA with a molar mass of M_w = 1800 g mol^{-1} (catalog number 323667-250g) from Sigma-Aldrich, and ethylene glycol and sodium hydroxide from Merck. For purification, Milli-Q grade (18.2 MΩ at 25 °C) water was used.

Synthesis. Silver nanoparticles were produced by adapting the polyol synthesis of our previous work on a silver catalyst.[7] By contrast, it was necessary to simplify that procedure to a one-pot synthesis for direct comparison of the conventional method with microwave heating. Silver nitrate (c = 32.4 g L^{-1}, solution 1) and PAA (c = 54 g L^{-1}, solution 2) were dissolved in ethylene glycol. A volume of 833 μL of solution 1 was added to 4.167 mL of solution 2 under stirring. Then, the reaction mixture was heated for particle formation, typically to 200 °C for 15 min. The particles were washed by adding 11.4 mL of water and allowing the particles to settle down. The supernatant was then removed after 24 h. This procedure was repeated twice. Thereafter, the residue was filled with water to 5 mL, and an aqueous sodium hydroxide solution (1 w/v

Received: May 7, 2017
Revised: November 28, 2017
Published: December 7, 2017

DOI: 10.1021/acs.langmuir.7b01541
Langmuir 2018, 34, 147−153

%) was added dropwise to disperse the nanoparticles. We used microwave glass vessels and glass flasks with a volume of 10 mL for synthesis. The conventional syntheses were carried out also as a one-pot synthesis in an oil bath. Each vessel was inserted quickly into the hot oil bath to imitate the rapid heating rates available in microwave synthesis.

DLS Measurements. The DLS measurements were performed using a multiangle ALV 7004 device from ALV Langen, equipped with a He−Ne laser (wavelength = 632.8 nm). The samples were diluted using an aqueous sodium hydroxide solution (pH = 10) in a ratio of 1:100 and filtrated using a Millex-LCR syringe filter (450 nm pores, hydrophilic polytetrafluoroethylene). Measurements were performed at scattering angles of $2\theta = 26°$—146 °C in 8° steps at a temperature of 23 ± 1 °C. Six measurement runs with 60 s for each angle were performed. The method of cumulants according to standard ISO 13321:1996 was used for the determination of the hydrodynamic radii at different angles. Realistic values for R_h can be obtained when the polydispersity index (PDI) is lower than 0.1. The PDI is the ratio of the variance of the relaxation rates (second cumulant μ) and the square of the mean relaxation rate (first cumulant $\bar{\Gamma}$). Plots of $1/R_h$ as a function of q^2 were used to investigate whether a higher dispersity and/or aggregation of the samples are present.[8]

SAXS Measurements. SAXS measurements were performed in a flow through capillary with a Kratky-type instrument (SAXSess from Anton Paar, Austria) at 21 ± 1 °C. Samples analyzed by SAXS were used as prepared. The measured intensity was converted to the absolute scale, according to Orthaber et al.[9] The scattering vector q depends on the wavelength λ of the radiation (λ = 0.154 nm): thus, $q = 4\pi/\lambda \sin\theta$. Deconvolution (slit length desmearing) of the SAXS curves was performed with the SAXS-Quant software (Anton Paar, Austria). Curve fitting was conducted with the software McSAS (version 1.0.1).[10] Because the scattering intensity was measured on an absolute scale, the volume fraction of the particles was determined in addition to the particles' volume weighted radii distribution when applying McSAS. The yields were calculated as the ratio of the experimentally determined volume fraction to the maximal possible volume fraction. The latter is calculated from the mass of silver which forms if all silver ions would have been reduced. Furthermore, we assumed that the density of the silver particles is the same as silver in the bulk form (10.49 g cm^{-3}).

RESULTS AND DISCUSSION

One-Pot Particle Synthesis. We adapted a widely used polyol synthesis[6] for particle formation with PAA as the stabilizer close to our previously published protocol.[7] Originally, a hot injection method is employed. This procedure had to be modified because no substances could be added during operation of the microwave. Therefore, all compounds were mixed at 20 °C immediately before microwave heating. The compounds were dissolved in ethylene glycol, identical to the procedure for conventional heating synthesis. The resultant raw product was transferred from ethylene glycol to water using the same purification procedure for both the synthesis methods (see the Experimental Section).

The vessel material presents a possible factor influencing the reaction pathway in a microwave reactor because of the material-dependent microwave absorption properties. Borosilicate glass exhibits a minimal absorption of microwave radiation, while silicon carbide (SiC) absorbs strongly.[11] Hence, a homogeneous heating of ethylene glycol as the reaction medium in borosilicate glass can be expected, whereas in silicon carbide, heating via heat conduction from the vessel walls occurs.[11] Because of this difference, we investigated the influence of the vessel material on the resulting particle characteristics.

Microwave and Conventional Heating Syntheses at 200 °C. For the comparison of microwave and conventional syntheses, we applied the same conditions as in our previous protocol: a reaction time of 15 min at a temperature of 200 °C. Before purification, the mean radius of the resulting particles does not significantly differ in dependence of the used glass vessel. The particles were characterized as synthesized in ethylene glycol by SAXS. Typical scattering curves and curve fits are shown in Figure 1a. The corresponding size distributions were approximated with Gaussian distributions (bars and solid lines in Figure 1b). Conventional heating synthesis using a borosilicate vessel yielded particles with a mean radius of R = 3.0 ± 0.1 nm and a size distribution width of σ = 0.6 ± 0.1 nm. Control experiments using a regular laboratory glass flask for conventional heating synthesis resulted in particles with the same values (not shown). For particles prepared via microwave-assisted synthesis, we found R = 3.3 ± 0.1 nm and σ = 0.7 ± 0.1 nm when using a borosilicate glass vessel. The values were R = 3.7 ± 0.1 nm and σ = 0.7 ± 0.1 nm for synthesis in vessels made of SiC.

We transferred the nanoparticles from ethylene glycol to water (see the Experimental Section). For the conventionally synthesized particles, we obtained R = 3.1 ± 0.1 nm and σ = 0.6 ± 0.1 nm derived by SAXS measurements (Figure 1c,d). Microwave-synthesized particles using a microwave glass vessel exhibited values of R = 3.4 ± 0.1 nm and σ = 0.7 ± 0.1 nm. For the particles synthesized in SiC vessels, we found R = 3.7 ± 0.1 nm with σ = 0.7 ± 0.1 nm. As a first conclusion, we state that there is no significant difference in the particle core characteristics between conventional and microwave-assisted syntheses when the same vessels made of borosilicate glass are used (Figure 2). Tendentially, the usage of SiC vessels results in particles with slightly larger core radii but a similar size distribution. Therefore, neither the heating method nor the vessel material has a substantial influence on the silver nanoparticles' core size. This indicates that the method is surprisingly robust against variations of the synthesis details. This is furthermore confirmed by identical UV/vis-spectra (Figure 1e). Each synthesis type results in particles with an absorption maximum at 413 ± 3 nm.

Because of its comparably weak scattering, the PAA shell is practically invisible in SAXS. Therefore, we performed multi-angle dynamic light scattering for determination of the hydrodynamic radii of the particles in aqueous solution. As the hydrodynamic radius includes the particles' silver core and their polymeric shell, R_h should be larger than the core radii derived from SAXS. We found that the reciprocal hydrodynamic radii $1/R_h$ were independent of the square of the scattering vector q^2 as shown in Figure 3 (data are given as symbols and straight lines are mean values). This leads us to the conclusion that particles from all syntheses are free of aggregates.[8] The hydrodynamic radius of the particles from conventional heating synthesis is R_h = 6.9 ± 0.1 nm with a PDI of 0.11 ± 0.05. The particles resulting from microwave synthesis show a hydrodynamic radius of R_h = 7.6 ± 0.2 nm and PDI = 0.11 ± 0.02 for the microwave glass vessel and R_h = 9.4 ± 0.1 nm and PDI = 0.12 ± 0.02 for the SiC vessel. Estimates of the shell thickness as $R_{shell} = R_h - R$ results in R_{shell} = 3.8 ± 0.2 nm (conventional heating), 4.2 ± 0.3 nm (microwave heating in glass), and 5.7 ± 0.2 nm (microwave heating in SiC). These values indicate that the particle shell thickness depends on the type of heating, that is, it is slightly larger for microwave-assisted synthesis. This is in contrast to the heat-type independent core size of the particles. However, carrying out this modified one-pot particle synthesis at 200 °C for 15 min in glass vessels yielded reproducible particle systems irrespective of the heating source and vessel form. The utilization of SiC vessels seems to have stronger impact on the distribution parameters (Table 1.

DOI: 10.1021/acs.langmuir.7b01541
Langmuir 2018, 34, 147−153

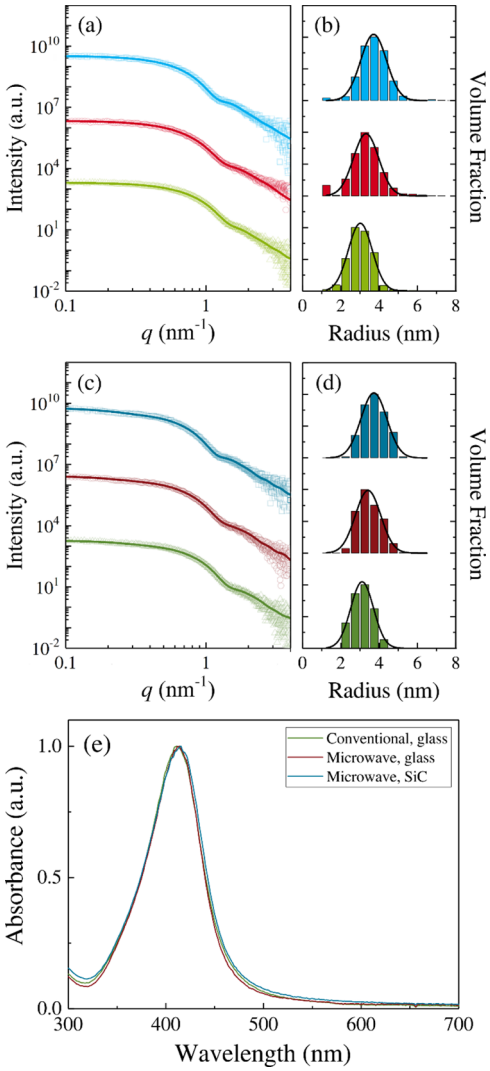

Figure 1. (a) SAXS data (symbols) and curve fits (solid lines) of silver nanoparticles as synthesized in ethylene glycol. Particles were prepared via conventional heating (glass vessel, green triangles) and via microwave-assisted heating (glass vessel, red circles and SiC vessel, blue squares). The curve fits in (a) correspond to the size distributions shown in (b) (bars). Gaussian fits of the histograms (solid lines) provide mean radii of $R = 3.0 \pm 0.1$ nm and size distribution widths of $\sigma = 0.6 \pm 0.1$ nm for conventional heating (green bars). Values for microwave-assisted synthesis are $R = 3.3 \pm 0.1$ nm and $\sigma = 0.7 \pm 0.1$ nm when a borosilicate glass vessel (red bars) was used and $R = 3.7 \pm 0.1$ nm and $\sigma = 0.7 \pm 0.1$ nm for synthesis in SiC vessels (blue bars). (c) SAXS data (symbols) and fits (solid lines) of the same silver nanoparticles as in (a) after their transfer from ethylene glycol to water. (d) Curve fits in (c) correspond to the size distributions shown in (d) (bars). The size characteristics are $R = 3.1 \pm 0.1$ nm and $\sigma = 0.6 \pm 0.1$ nm for conventional heating (green). For microwave heating, the values are $R = 3.4 \pm 0.1$ nm and $\sigma = 0.7 \pm 0.1$ nm when a the borosilicate glass vessel was used (red) and $R = 3.7 \pm 0.1$ nm and $\sigma = 0.7 \pm 0.1$ nm when SiC was used as the vessel material (blue). The scattering curves in (a,c) were shifted vertically for better visibility. (e) UV/vis-spectra of silver nanoparticles formed via conventional heating in a glass vessel and via microwave heating in a glass vessel as well as in a SiC vessel (green, red, and blue solid line, respectively).

High-Speed Syntheses. Because we wanted to take advantage of performing microwave synthesis at a high reaction rate, we investigated the results of the synthesis in terms of particle size and yield at different temperatures for a constant reaction time of 3 min. To study the particle formation process of our system, the syntheses were carried out first below the boiling temperature of ethylene glycol (197.5 °C) at 150 °C and then at temperatures of 200, 250, and 300 °C. The corresponding pressure values were 1, 1, 4, and 11 bar, respectively.

We found no particle formation at a reaction temperature of 150 °C. This is in accordance with our expectation because the polyol process is initiated once the boiling temperature of ethylene glycol is reached.[6] Then, oxidative decomposition of ethylene glycol results in the reduction of silver ions forming silver atoms. These atoms first coalesce successively to silver clusters and further to nanoparticles probably following the particle formation mechanism described by Polte et al.[12] At a reaction temperature of 200 °C, particles were formed but the reaction yield shows an incomplete turnover of the silver ions within 3 min of heating. The formed particles exhibited a mean radius of $R = 2.3 \pm 0.1$ nm and a distribution width of $\sigma = 0.6 \pm 0.1$ nm (Figure 4a). The reaction was incomplete with a particle yield of 86 ± 5% (Figure 4b). The size characteristics of the particles produced at 250 °C, as synthesized in ethylene glycol, are $R = 3.7 \pm 0.1$ nm and $\sigma = 0.9 \pm 0.1$ nm. For the particle synthesis at 300 °C, we determined $R = 4.1 \pm 0.1$ nm and $\sigma = 1.1 \pm 0.1$ nm. The yields of 94 ± 5% for 250 °C and 98 ± 5% for 300 °C indicate that the reaction was completed at both temperatures within 3 min.

We transferred the batches with complete yield from ethylene glycol to water and found that the particle size characteristics remain constant (see Figure 4a). Surprisingly, the 200 °C batch with the uncompleted reaction cannot be transferred from ethylene glycol to water. Probably, remaining silver ions, which are present from the incomplete conversion of Ag^+ to Ag^0 after 3 min at 200 °C are causing this behavior. One may speculate that Ag^+ ions adsorbed onto the PAA-covered silver nanoparticle surface prevent the solvent transfer. The particles synthesized at 250 and 300 °C display product losses resulting from the transfer procedure of 16 ± 2 and 88 ± 10%, respectively (Figure 4b). Thereby, the former value represents an acceptable result for a purification procedure in contrast to the latter one. A partial degradation of PAA at a temperature of 300 °C might lead to the high product loss. Thermal degradation investigations of PAA support this assumption.[13]

DLS measurements of the purified particles display hydrodynamic radii within a range of 8−11 nm without significant dependence on the temperature used for the microwave synthesis. The PDIs are tendentially lower when the synthesis was performed at 250 °C (PDI = 0.19 ± 0.02) than at 300 °C (0.28 ± 0.02).

The formation of larger particles with increasing temperature as schematically depicted in Figure 4c is surprising on the first sight. Intuitively, one expects that the higher the temperature, the higher is the number of seeds from which the particles grow, and therefore, the final particle size should decrease with increasing temperature. However, if we consider a mechanism of coalescence of silver clusters, more clusters coalesce at higher temperatures to form a nanoparticle. Therefore, we assume temperature-dependent cluster coalescence as a dominating mechanism to explain the difference in the particle size. Clark et al.[14] provided a theoretical description on controlling the size distribution of nanocrystals via the production conditions. However, a detailed experimental comparison with their theory is beyond the scope of the present work.

Minimizing the Reaction Time. The findings above suggest that a microwave reaction temperature of 250 °C is an optimum

DOI: 10.1021/acs.langmuir.7b01541
Langmuir 2018, 34, 147−153

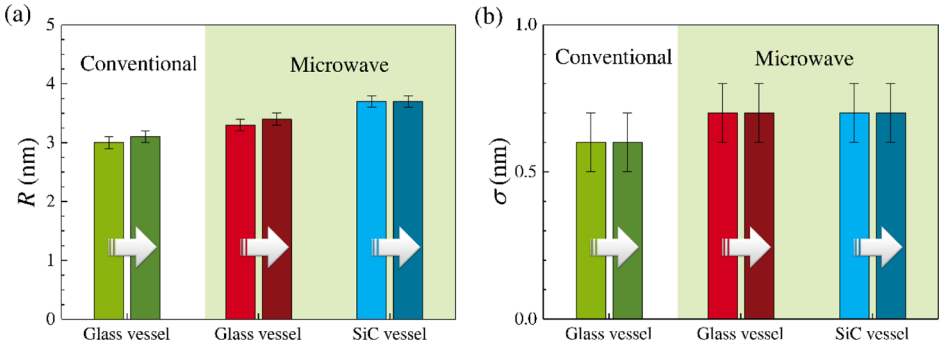

Figure 2. SAXS-derived characteristics of silver nanoparticles prepared via conventional and microwave-assisted heating in reaction vessels made of borosilicate glass and SiC, respectively. Shown are (a) mean radii R and (b) distribution widths σ of particles in ethylene glycol (raw product) and water (purified product) displayed as left and right bars, respectively (purification indicated by arrows).

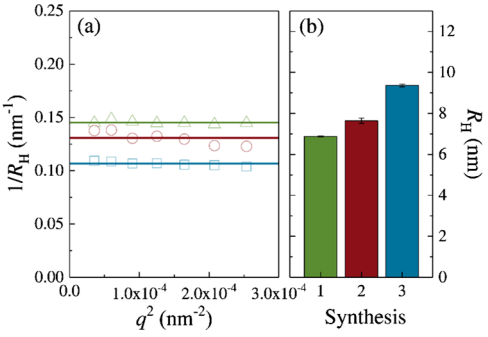

Figure 3. DLS results for silver nanoparticles prepared via conventional heating (green) and microwave heating in glass and SiC vessels (red and blue, respectively) after transfer from ethylene glycol to aqueous solution. (a) Reciprocal values of the hydrodynamic radii as a function of q^2 (symbols) are constant (solid lines). (b) Fits shown in panel (a) result in $R_h = 6.9 \pm 0.1$ nm (synthesis 1, conventional heating), $R_h = 7.6 \pm 0.2$ nm (synthesis 2, microwave heating, glass), and $R_h = 9.4 \pm 0.1$ nm (synthesis 3, microwave heating, SiC).

Table 1. Characteristics of Silver Nanoparticle Systems from Synthesis via Conventional and Microwave Heating[a]

synthesis	1	2	3
type of heating	conventional	microwave	microwave
reaction vessel	glass	glass	SiC
Particles Dispersed in Ethylene Glycol (Raw Product As-Prepared)			
R [nm]	3.0 ± 0.1	3.3 ± 0.1	3.7 ± 0.1
σ [nm]	0.6 ± 0.1	0.7 ± 0.1	0.7 ± 0.1
Particles Dispersed in Water (Purified Product, After Transfer from Ethylene Glycol)			
R [nm]	3.1 ± 0.1	3.4 ± 0.1	3.7 ± 0.1
σ [nm]	0.6 ± 0.1	0.7 ± 0.1	0.7 ± 0.1
R_h [nm]	6.9 ± 0.1	7.6 ± 0.2	9.4 ± 0.1
PDI	0.11 ± 0.05	0.11 ± 0.02	0.12 ± 0.02
R_{shell} [nm]	3.8 ± 0.2	4.2 ± 0.3	5.7 ± 0.2

[a]Types of reaction vessels were borosilicate glass (synthesis number 1 and 2) and silicon carbide (SiC, synthesis 3). The particle core radii, R, and their size distribution widths, σ, of particles in ethylene glycol and after their transfer to water were determined by SAXS. The hydrodynamic radii, R_h, and the PDIs of particles in aqueous solution were determined by DLS. The shell thickness, R_{shell}, was calculated as $R_h - R$.

in terms of particle yield for three minute syntheses. Reducing the reaction time further to a minimum of 30 s still led to a complete conversion. The particle size distribution parameters are nearly identical and do not significantly change upon purification. In comparison, mean radii of $R = 3.3 \pm 0.1$ nm (200 °C) and $R = 3.4 \pm 0.1$ nm (250 °C) before purification as well as $R = 3.6 \pm 0.1$ nm (200 and 250 °C) after purification are obtained (Figure 5a). The distribution widths before and after purification amount to $\sigma = 1.0 \pm 0.1$ nm (200 °C) and $\sigma = 0.8 \pm 0.1$ nm (250 °C). The scattering patterns of the purified systems are highly comparable as shown in an overlay of the data in Figure 5b. Thus, we can state that the particle synthesis in a microwave can be effectively accelerated by increasing the temperature by 50 K without affecting the size distribution parameters.

The Arrhenius equation describes the relation between the reaction rate constant k_i and the temperature T_i via the pre-exponential factor A, energy of activation E_a, and the universal gas constant R as $k_i = A \exp\left[-\frac{E_a}{RT_i}\right]$. At two different temperatures, T_2 and T_1, the corresponding reaction rate constants are $k_2 = A \exp\left[-\frac{E_a}{RT_2}\right]$ and $k_1 = A \exp\left[-\frac{E_a}{RT_1}\right]$. The ratio of the reaction rate constants is $\frac{k_2}{k_1} = \exp\left[\frac{E_a}{R}\left(\frac{1}{T_1} - \frac{1}{T_2}\right)\right]$ from which the activation energy can be estimated as

$$E_a = \frac{R\, T_1 T_2 \ln(k_2/k_1)}{T_2 - T_1} \quad (1)$$

For an increase of the temperature from $T_1 = 200$ °C to $T_2 = 250$ °C, we found a decrease in the reaction time of $t_2 \approx t_1/30$. Because the educts and the products did not change for the different reaction times t_i, we assume that the product of the reaction time and speed is the same for both syntheses. Hence, we can estimate that the ratio of the reaction times t_1/t_2 is the same as the ratio of the reaction rate constants k_2/k_1. According to eq 1, we calculated an activation energy of $E_a \approx 139$ kJ mol^{-1}. This value seems to be reasonable because it is between the reported dissolution energy of 69 kJ mol^{-1} for silver nanoparticles[14] and the activation energy of 174 kJ mol^{-1} reported for the growth of silver nanoparticles.[15]

Particle Growth by Incubation at Elevated Temperatures. In nanoparticle synthesis, the exact tuning of the particle parameters is of high importance. Because the silver particle formation is certainly completed after 3 min at 300 °C, the question arises whether it is possible to fine-tune the particle radius with a subsequent growth phase. Because of increasing pressure values at 300 °C, the temperature was lowered to 250 °C after 3 min to allow further growth of the particles for 12 min.

Indeed, larger particles with $R = 7.1 \pm 0.1$ nm and $\sigma = 2.6 \pm 0.1$ nm were obtained (Figure 6a). As shown above, the conversion

DOI: 10.1021/acs.langmuir.7b01541
Langmuir 2018, 34, 147−153

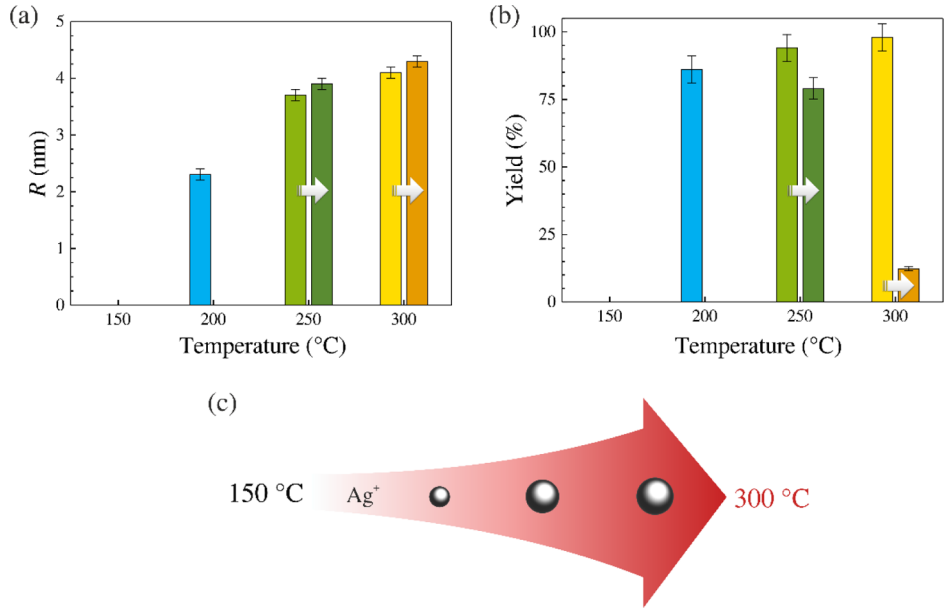

Figure 4. Three minute synthesis at different temperatures (150, 200, 250, and 300 °C). Comparison of (a) mean radii R and (b) product yield before and after purification (left and right bars, respectively). (c) Scheme of the increasing particle size with the increasing reaction temperature.

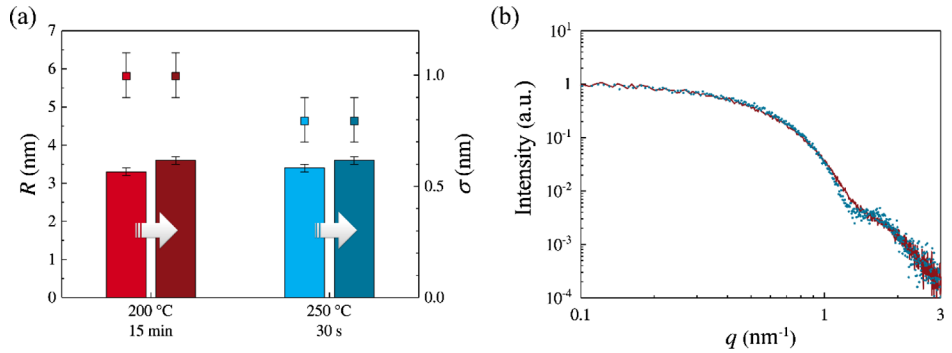

Figure 5. (a) Mean radii R (bars) and the distribution widths σ (symbols). Arrows indicate parameters before and after purification of the particles. (b) Overlay of the scattering curves from particles synthesized for 15 min at 200 °C and for 30 s at 250 °C with microwave heating after purification (red solid line and blue dotted line, respectively). The curves were normalized to unity for better comparison.

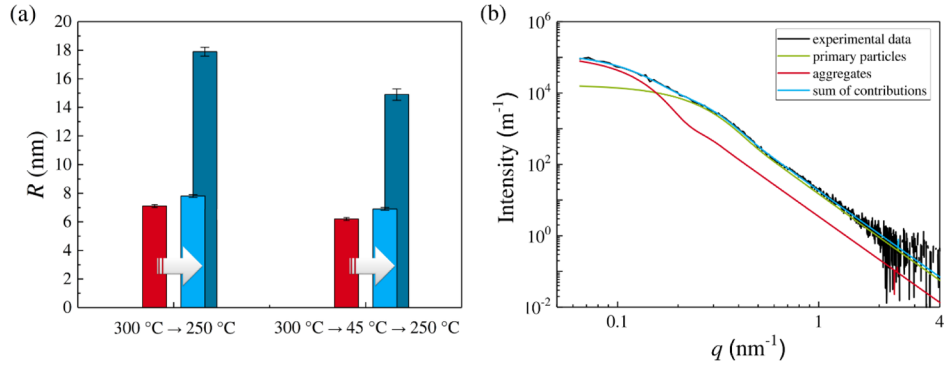

Figure 6. (a) Comparison of the mean radii R after subjecting the reaction mixture to the denoted temperature sequence, before (left red bar for each temperature sequence) and after purification (right bars for each temperature). After purification, the particle systems are consisting of a mixture of primary particles (bright blue bar in the middle) and aggregates (dark blue bar on the right). (b) Scattering curve of the particles produced by the temperature sequence 300 °C → 45 °C → 250 °C (black), and the curve fit (blue) composed of the contribution of primary particles (green) and aggregates (red).

of silver ions to elementary silver is certainly completed after 3 min at 300 °C forming particles with $R = 4.1 \pm 0.1$ nm and $\sigma = 1.1 \pm 0.1$ nm. Therefore, we conclude that the 12 min incubation at 250 °C led to a particle growth by approximately 3 nm, which was accompanied by a broadening of the size distribution. It is not clear whether this growth is caused by Ostwald ripening or coalescence because both processes are experimentally challenging to distinguish from each other.[16] According to LaMer's

DOI: 10.1021/acs.langmuir.7b01541
Langmuir 2018, 34, 147−153

principle of particle formation, the separation of nucleation and particle growth is a crucial factor for the production of particles with a narrow size distribution. To achieve a better separation of the initial synthesis at 300 °C and the subsequent growth phase, a short cooling to 45 °C was inserted. The resulting particles were slightly smaller (R = 6.2 ± 0.1 nm) and have a narrower size distribution width (σ = 2.1 ± 0.1 nm) than those obtained without intermediate cooling (Figure 6a). Unfortunately, aggregates were present after transfer from ethylene glycol to water. This is reflected in R_h values of 20.1 ± 0.4 nm (without cooling) and 25.5 ± 2.2 nm (with cooling) as well as PDIs of 0.33 ± 0.02 and 0.30 ± 0.01, respectively. We assume that this is mainly caused by a partial decomposition of the stabilizing PAA. Interpretation of the SAXS data shows that a mixture of primary particles and aggregates is present after transfer. In the first case (12 min incubation at 250 °C), the primary particles display a core radius of 7.8 ± 0.1 nm and the aggregates' radius amounts to 17.9 ± 0.3 nm. The data, the curve fit, and the contribution of primary particles and aggregates are shown in Figure 6b. From the relative intensities of the scattering contributions, we calculate a number ratio of primary particles to aggregates of 60 to 1. From the volume ratio of aggregates to primary particles, we estimate an aggregation number of about 12 primary particles per aggregate. In the second case (inserted short cooling to 45 °C), the primary particles display a core radius of 6.9 ± 0.1 nm, and the aggregates' radius is 14.9 ± 0.4 nm. The relative intensities of the scattering contributions allow the determination of the number ratio of primary particles to aggregates of 44 to 1. The volume ratio of aggregates to primary particles leads to an aggregation number of about 10 primary particles per aggregate.

Therefore, we conclude that silver nanoparticles can be further grown by a postsynthetic heating step. A remaining crucial challenge lies in getting a better control over the dispersity, which can be at least reduced by intermediate cooling between particle synthesis and growth phase.

CONCLUSIONS

Our work demonstrates that ultra-small silver nanoparticles with 3 nm radius and a narrow size distribution can be produced in a one-pot reaction via conventional as well as microwave synthesis. Thereby, the heating source and the vessel type have no substantial impact on the particle core size. By contrast, a dependence of the particle shell thickness on the heating type is found, that is, microwave-assisted syntheses result in larger hydrodynamic radii. The particle size increases in dependence of the temperature while the reaction time was held constant. Therefore, we assume that the growth of the silver nanoparticles is dominated by a temperature-dependent cluster coalescence mechanism. By increasing the reaction temperature by 50 K, the reaction time can be effectively reduced by 97%. An estimate of the activation energy derived from the increasing reaction rate amounts to 139 kJ mol^{-1}. As a consequence of the high temperature and the corresponding high pressure, this reaction pathway is only accessible in pressurized environments, that is, microwave reactors. While the particle parameters derived from SAXS and DLS show no significant change, the particle losses during purification increase with the increasing temperature. This implies that time- and material-saving reaction routes have to be weighed up against each other. Subsequent heating and therefore longer reaction times at elevated temperatures lead to particle growth via Ostwald ripening or coalescence, which gives the opportunity of tuning the particle size. However, a better control over the dispersity has to be achieved. Potential specific or nonthermal microwave effects could not be observed during these experiments.

AUTHOR INFORMATION

Corresponding Author

*E-mail: andreas.thuenemann@bam.de. Phone: +493081041610.

ORCID

Patrick E. J. Saloga: 0000-0003-4794-2188

Claudia Kästner: 0000-0003-3730-7404

Andreas F. Thünemann: 0000-0002-9883-6134

Author Contributions

†P.E.J.S. and C.K. contributed equally to this work.

Notes

The authors declare no competing financial interest.

ACKNOWLEDGMENTS

We thank M. Ebisch for help in synthesis and H.V. Schröder for his thorough advice concerning graphics.

REFERENCES

(1) Baghbanzadeh, M.; Carbone, L.; Cozzoli, P. D.; Kappe, C. O. Microwave-Assisted Synthesis of Colloidal Inorganic Nanocrystals. *Angew. Chem., Int. Ed.* **2011**, *50*, 11312−11359.

(2) Nguyen, N. T.; Nguyen, B. H.; Ba, D. T.; Pham, D. G.; Khai, T. V.; Nguyen, L. T.; Tran, L. D. Microwave-Assisted Synthesis of Silver Nanoparticles Using Chitosan: A Novel Approach. *Mater. Manuf. Processes* **2014**, *29*, 418−421.

(3) Dzido, G.; Markowski, P.; Małachowska-Jutsz, A.; Prusik, K.; Jarzębski, A. B. Rapid continuous microwave-assisted synthesis of silver nanoparticles to achieve very high productivity and full yield: from mechanistic study to optimal fabrication strategy. *J. Nanopart. Res.* **2015**, *17*, 15.

(4) Soliveri, G.; Ardizzone, S.; Yüksel, S.; Cialla-May, D.; Popp, J.; Schubert, U. S.; Hoeppener, S. Microwave-Assisted Silver Nanoparticle Film Formation for SERS Applications. *J. Phys. Chem. C* **2016**, *120*, 1237−1244.

(5) Gedye, R. N.; Wei, J. B. Rate enhancement of organic reactions by microwaves at atmospheric pressure. *Can. J. Chem.* **1998**, *76*, 525−532.

(6) Hu, Y.; Ge, J.; Lim, D.; Zhang, T.; Yin, Y. Size-controlled synthesis of highly water-soluble silver nanocrystals. *J. Solid State Chem.* **2008**, *181*, 1524−1529.

(7) Kästner, C.; Thünemann, A. F. Catalytic Reduction of 4-Nitrophenol Using Silver Nanoparticles with Adjustable Activity. *Langmuir* **2016**, *32*, 7383−7391.

(8) Bantz, C.; Koshkina, O.; Lang, T.; Galla, H.-J.; Kirkpatrick, C. J.; Stauber, R. H.; Maskos, M. The surface properties of nanoparticles determine the agglomeration state and the size of the particles under physiological conditions. *Beilstein J. Nanotechnol.* **2014**, *5*, 1774−1786.

(9) Orthaber, D.; Bergmann, A.; Glatter, O. SAXS experiments on absolute scale with Kratky systems using water as a secondary standard. *J. Appl. Crystallogr.* **2000**, *33*, 218−225.

(10) Bressler, I.; Pauw, B. R.; Thünemann, A. F. McSAS: software for the retrieval of model parameter distributions from scattering patterns. *J. Appl. Crystallogr.* **2015**, *48*, 962−969.

(11) Kappe, C. O. Unraveling the Mysteries of Microwave Chemistry Using Silicon Carbide Reactor Technology. *Acc. Chem. Res.* **2013**, *46*, 1579−1587.

(12) Polte, J.; Tuaev, X.; Wuithschick, M.; Fischer, A.; Thünemann, A. F.; Rademann, K.; Kraehnert, R.; Emmerling, F. Formation Mechanism of Colloidal Silver Nanoparticles: Analogies and Differences to the Growth of Gold Nanoparticles. *ACS Nano* **2012**, *6*, 5791−5802.

(13) Lu, X.; Tan, C. Y.; Xu, J.; He, C. Thermal degradation of electrical conductivity of polyacrylic acid doped polyaniline: effect of molecular weight of the dopants. *Synth. Met.* **2003**, *138*, 429−440.

DOI: 10.1021/acs.langmuir.7b01541
Langmuir 2018, 34, 147−153

(14) Clark, M. D.; Kumar, S. K.; Owen, J. S.; Chan, E. M. Focusing Nanocrystal Size Distributions via Production Control. *Nano Lett.* **2011**, *11*, 1976−1980.
(15) Jiménez, J. A.; Sendova, M. Kinetics of Ag nanoparticle growth in thick SiO2 films: An in situ optical assessment of Ostwald ripening. *Mater. Chem. Phys.* **2012**, *135*, 282−286.
(16) Liebig, F.; Thünemann, A. F.; Koetz, J. Ostwald Ripening Growth Mechanism of Gold Nanotriangles in Vesicular Template Phases. *Langmuir* **2016**, *32*, 10928−10935.

DOI: 10.1021/acs.langmuir.7b01541
Langmuir 2018, 34, 147−153